Linearization of Active Array Transmitters Under Crosstalk via Over-the-Air Observations

Joel Fernandez*, Lauri Anttila*, Mikko Valkama*, and Thomas Eriksson†
*Unit of Electrical Engineering, Tampere University, Tampere, Finland,
†Department of Electrical Engineering, Chalmers University of Technology, Gothenburg, Sweden,
{joel.fernandez, lauri.anttila, mikko.valkama}@tuni.fi, thomase@chalmers.se

***Abstract*—Finding computationally feasible solutions to linearize active antenna array transmitters is a timely challenge in modern cellular networks, particularly in 5G and the emerging 6G systems. In this paper, we propose a new modeling and parameter estimation approach to characterize the individual power amplifier (PA) units of an active antenna array subject to crosstalk while relying only on over-the-air observations. Additionally, we describe a beam-sweeping based forward model learning procedure and the corresponding closed-loop digital predistortion (DPD) learning algorithm, to efficiently linearize millimeter-wave phased-array transmitters under crosstalk-induced load modulation. The provided numerical results demonstrate excellent parameter estimation and linearization performance, reaching adjacent channel power ratios (ACPRs) as low as –50 to –60 dB with realistic evaluation assumptions.**

***Index Terms*—5G, 6G, active array transmitters, antenna crosstalk, digital predistortion, linearization, power-efficiency**

I. Introduction

The ability to achieve good power-efficiency while still meeting the stringent transmit waveform quality requirements is one of the most important implementation challenges in modern radio communication systems, such as the 5G New Radio (NR) [1], [2]. To this end, digital predistortion (DPD) [3], [4] is the most common approach for mitigating the power amplifier (PA) induced nonlinear distortion, particularly in cellular base-stations. When properly applied, DPD technology allows pushing the PAs closer towards their saturation region, and hence achieving largely improved power-efficiency, while still meeting the transmitter error vector magnitude (EVM) and out-of-band (OOB) emission requirements. This is also the main technical scope of this paper, with specific emphasis on modern *active antenna array transmitters*.

In the context of active antenna arrays and beamforming networks, the current state-of-the-art DPD solutions [5]–[10] concentrate on computationally feasible processing and learning architectures that allow for simultaneously linearizing multiple and mutually different PAs. Most of the reported array DPD solutions, especially in millimeter-wave (mmWave) networks, rely on measuring or building the so-called main-beam observation signal, which is used as the basis for DPD parameter learning. In such a beamformed domain, a traditional single-input–single-output DPD learning problem is effectively obtained, which yields the technical basis to linearize the main-beam signal [6]. In terms of the practical feedback or observation receiver arrangements [5], [10], two alternative approaches have been considered. The first one is a classical conductive approach, where the individual PA output signals are measured through directional couplers. The second approach relies on over-the-air (OTA) feedback, with external observation receiver(s). The classical conductive approach requires couplers for each transmit PA/antenna path which may not be feasible – especially in mmWave systems – hence, the emphasis is more towards the OTA approaches.

An additional important challenge in any array or multiple-input multiple-output (MIMO) transmitter is the crosstalk and other interactions between the antennas. In the linearization context, this is known to result in beam-dependent nonlinear behavior due to the load modulation phenomenon [1]. Furthermore, in digital array/MIMO transmitter scenarios, the crosstalk can largely degrade the performance of ordinary single-input DPD models, and hence different more evolved multi-dimensional polynomial-based linearization models have been proposed [11]–[13]. However, the complexity of such multi-dimensional models grows really aggressively with the number of TX chains, and thus they can be seen as feasible only with a small number of TX paths. To alleviate the complexity issue, [14] proposed a novel dual-input DPD architecture along with a proper crosstalk model that allows linearizing the TX efficiently with more favorable complexity.

In this paper, we address the challenging problems of linearization and parameter estimation of nonlinear active antenna arrays under crosstalk via over-the-air observations. Compared to the existing state-of-the-art literature, the main contributions of the paper can be described as follows:

- We derive and provide an explicit nonlinear array transmitter model with detailed insight on crosstalk and no-crosstalk conditions, applicable to arbitrary array/MIMO scenarios. Such explicit model makes numerical evaluations and assessment of nonlinear active arrays more straight-forward, compared to the existing implicit dual-input PA/transmitter models.
- We develop and propose a novel parameter identification approach and algorithm for arbitrary array/MIMO transmitters under crosstalk, to characterize the individual PA units and their nonlinearities while utilizing only OTA observations.

This work was supported in part by the Academy of Finland under grants #319994, #323461, #338224, and #332361, and in part by Business Finland and Vinnova under the "Energy-Efficient Radio Systems at 100 GHz and Beyond: Antennas, Transceivers and Waveforms (ENTRY100GHz)" project.

- We then apply the modeling and parameter identification methods in a practical mmWave phased-array transmitter context, where a selected subset of the antenna units are used for observation purposes through physical coupling.
- We develop and describe an efficient direct learning approach for estimating the phased-array single-input DPD coefficients where the involved forward-path non-linear array model coefficients are obtained using the above-proposed parameter identification approach.
- We provide a large collection of numerical results, demonstrating the excellent nonlinear forward model estimation accuracy as well as the corresponding phased-array linearization performance while varying the fundamental system parameters such as the estimation signal-to-noise ratio (SNR), the amount of the parameter estimation samples, and the PA forward model order.

The rest of this paper is organized as follows. First, the active array linearization-related system model is described in Section II. Then, the proposed nonlinear PA model identification approach is described in Section III, applicable to arbitrary active arrays. Then, the utilization of the nonlinear model for linearizing phased-arrays is considered and described in Section IV. In Section V, extensive numerical results are provided related to evaluating the performance of the proposed active array model identification and phased-array linearization techniques, while the conclusions are drawn in Section VI.

II. System Model

The considered system scenario is illustrated in Fig. 1. In the following, all models are expressed through complex-valued baseband equivalents in discrete-time domain. Additionally, for readability purposes, explicit time dependence is omitted such that, e.g., the signal $a_{1k}(n)$ is expressed as a_{1k}.

A. PA and Nonlinear Array Models

1) Implicit Expression for PA Output Signals: Using a complex dual-input polynomial structure [14], [15], the output signal of the k^{th} transmit path or PA can be described as

$$b_{2k} = \sum_{p=0}^{(P-1)/2} \alpha_{kp} a_{1k}^{(p+1)} {a_{1k}^*}^p + \sum_{p=0}^{(P-1)/2} \beta_{kp} a_{1k}^p {a_{1k}^*}^p a_{2k} + \sum_{p=1}^{(P-1)/2} \gamma_{kp} a_{1k}^{(p+1)} {a_{1k}^*}^{(p-1)} a_{2k}^*, \quad (1)$$

where α_{kp}, β_{kp}, γ_{kp} are the complex PA model coefficients, P is the polynomial order and $()^*$ refers to the complex conjugation. Denoting the coupling coefficients by λ_{ki}, the crosstalk signals are given as

$$a_{2k} = \sum_{i=1, i\neq k}^{K} \lambda_{ki} b_{2i}. \quad (2)$$

In practice, the coupling coefficients can be obtained, e.g., by measuring the scattering parameters (the S-parameters) of the antenna array.

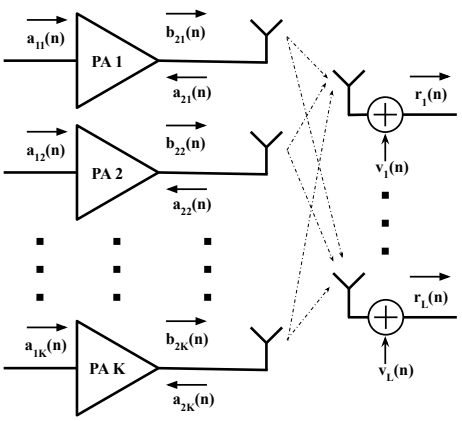

Fig. 1. Block diagram of a multi-antenna TX system model with K transmit paths. Each path consists of one PA unit connected to an antenna element.

It can be noted that the expressions in (1) and (2) are implicit in nature. Therefore, we next derive explicit expressions for the PA outputs, that are dependent only on the actual input signals. Through such explicit models, numerical evaluations and assessment of nonlinear array systems can be made substantially more straight-forward, compared to the implicit expressions in (1) and (2). This is one contribution of the paper.

2) Explicit Expression for PA Output Signals: To derive explicit expressions of the PA output signals under crosstalk, we switch to vector-matrix notations, and adopt the so called augmented modeling approach [16] where both the b_{2k}'s and b_{2k}^*'s are stacked together. To this end, for K transmit antennas, we first define two vectors $\mathbf{b} \in \mathbb{C}^{(2K\times 1)}$ and $\mathbf{d} \in \mathbb{C}^{(2K\times 1)}$ as $\mathbf{b} = [b_{21}\ b_{22}\ \cdots\ b_{2K}\ b_{21}^*\ b_{22}^*\ \cdots\ b_{2K}^*]^T$ and $\mathbf{d} = [d_1\ d_2\ \cdots\ d_K\ d_1^*\ d_2^*\ \cdots\ d_K^*]^T$, where

$$d_k = \sum_{p=0}^{(P-1)/2} \alpha_{kp} a_{1k}^{(p+1)} {a_{1k}^*}^p. \quad (3)$$

Then, by further defining $\mathbf{\Delta_{XY}} \in \mathbb{C}^{(2K\times 2K)}$ as

$$\mathbf{\Delta_{XY}} = \begin{bmatrix} \mathbf{X} & \mathbf{Y} \\ \mathbf{Y}^* & \mathbf{X}^* \end{bmatrix}, \quad (4)$$

where the elements of $\mathbf{X} \in \mathbb{C}^{(K\times K)}$ and $\mathbf{Y} \in \mathbb{C}^{(K\times K)}$ read

$$X_{kj} = \begin{cases} 1, & \text{if } k = j \\ -\lambda_{kj} \sum_{p=0}^{(P-1)/2} \beta_{kp} a_{1k}^p {a_{1k}^*}^p, & \text{if } k \neq j \end{cases} \quad (5)$$

and

$$Y_{kj} = \begin{cases} 0, & \text{if } k = j \\ -\lambda_{kj}^* \sum_{p=1}^{(P-1)/2} \gamma_{kp} a_{1k}^{(p+1)} {a_{1k}^*}^{(p-1)}, & \text{if } k \neq j \end{cases} \quad (6)$$

an explicit expression for $\mathbf{b}$ can be obtained through fairly straight-forward derivation steps, expressed eventually as

$$\mathbf{b} = (\mathbf{\Delta_{XY}})^{-1}\mathbf{d}. \quad (7)$$

As $\mathbf{b}$ is stacking both b_{2k}'s and b_{2k}^*'s, only the first K elements are eventually selected from $\mathbf{b}$. Note that X_{kj} and Y_{kj} are functions of β_{kp} and γ_{kp}, respectively. In the special

case of absence of load modulation, $\beta_{kp} = 0$ and $\gamma_{kp} = 0$, and thus $X_{kj} = 0$ and $Y_{kj} = 0\ \forall k \neq j$. In that case, $\mathbf{\Delta_{XY}}$ will be an identity matrix and $\mathbf{b} = \mathbf{d}$. Thus, as the load modulation in the system reduces, $\mathbf{\Delta_{XY}}$ converges to an identity matrix.

B. OTA Measurement Model

The assumed OTA observation model for the lth observation receiver, with $l = 1, 2, ..., L$, is expressed as

$$r_l = \sum_{k=1}^{K} \eta_{lk} b_{2k} + v_l \tag{8}$$

where v_l denotes complex additive white Gaussian noise (AWGN). In cases where some of the antenna units of the transmit array are used for observing through OTA coupling, as in Fig. 2 in the phased-array context, the channel coefficients η_{lk} can be assumed to be known. In practice, they can be obtained through S-parameters measurements of the antenna array, similar to the coupling coefficients λ_{ki}.

III. Proposed PA Model Identification Method

First, based on (1), the PA output of the k^{th} transmit path for N-sample sequences can be expressed in vector form as

$$\begin{aligned} \mathbf{b}_{2k} &= [\mathbf{G}^{(0)}(\mathbf{a}_{1k}) \quad \mathbf{G}^{(1)}(\mathbf{a}_{1k}, \mathbf{a}_{2k}) \quad \mathbf{G}^{(2)}(\mathbf{a}_{1k}, \mathbf{a}_{2k})] \\ &\quad \times [\boldsymbol{\alpha}_k^T \quad \boldsymbol{\beta}_k^T \quad \boldsymbol{\gamma}_k^T]^T \\ &= \mathbf{G}(\mathbf{a}_{1k}, \mathbf{a}_{2k})\boldsymbol{\theta}_k \end{aligned} \tag{9}$$

where $\mathbf{a}_{1k}$, $\mathbf{a}_{2k}$ and $\mathbf{b}_{2k}$ are complex-valued $(N \times 1)$ vectors containing sequences of N samples of the signals a_{1k}, a_{2k} and b_{2k}, e.g., $\mathbf{a}_{1k} = [a_{1k}(0), ..., a_{1k}(N-1)]^T$. The vectors $\boldsymbol{\alpha}_k \in \mathbb{C}^{(Q\times 1)}$, $\boldsymbol{\beta}_k \in \mathbb{C}^{(Q\times 1)}$, $\boldsymbol{\gamma}_k \in \mathbb{C}^{((Q-1)\times 1)}$, and $\boldsymbol{\theta}_k \in \mathbb{C}^{((3Q-1)\times 1)}$ contain the PA model coefficients, where $Q = (P-1)/2+1$ and $\mathbb{C}^{(A\times B)}$ denotes a complex-valued matrix of size $A \times B$. The matrices $\mathbf{G}(.)$ contain the corresponding basis functions, such that $\mathbf{G}^{(0)}(\mathbf{a}_{1k}) \in \mathbb{C}^{(N\times Q)}$, $\mathbf{G}^{(1)}(\mathbf{a}_{1k}, \mathbf{a}_{2k}) \in \mathbb{C}^{(N\times Q)}$, $\mathbf{G}^{(2)}(\mathbf{a}_{1k}, \mathbf{a}_{2k}) \in \mathbb{C}^{(N\times (Q-1))}$, and $\mathbf{G}(\mathbf{a}_{1k}, \mathbf{a}_{2k}) \in \mathbb{C}^{(N\times (3Q-1))}$.

Combining now (9) with the observation model in (8), a total system model for length N sequences with $L \geq 2$ observation receivers and K transmit paths is obtained. To this end, the observed sequences can now be expressed as

$$\mathbf{r} = \mathbf{F}\boldsymbol{\theta} + \mathbf{v}, \tag{10}$$

where

$$\mathbf{F} = \begin{bmatrix} \eta_{11}\mathbf{G}(\mathbf{a}_{11}, \mathbf{a}_{21}) & \dots & \eta_{1K}\mathbf{G}(\mathbf{a}_{1K}, \mathbf{a}_{2K}) \\ \vdots & \ddots & \vdots \\ \eta_{L1}\mathbf{G}(\mathbf{a}_{11}, \mathbf{a}_{21}) & \dots & \eta_{LK}\mathbf{G}(\mathbf{a}_{1K}, \mathbf{a}_{2K}) \end{bmatrix} \tag{11}$$

while $\mathbf{r} = [\mathbf{r}_1{}^T \dots \mathbf{r}_L{}^T]^T$ and $\mathbf{v} = [\mathbf{v}_1{}^T \dots \mathbf{v}_L{}^T]^T$ are complex-valued vectors of size $LN \times 1$. Additionally, $\boldsymbol{\theta} = [\boldsymbol{\theta}_1^T \dots \boldsymbol{\theta}_K^T]^T \in \mathbb{C}^{(K(3Q-1)\times 1)}$ and $\mathbf{F} \in \mathbb{C}^{LN\times (K(3Q-1))}$.

Finally, an estimate of the total parameter vector $\boldsymbol{\theta}$ can be obtained as a least squares solution of (10), expressed as

$$\hat{\boldsymbol{\theta}} = \mathbf{F}^{\dagger}\mathbf{r}, \tag{12}$$

where $\mathbf{F}^{\dagger}$ is the pseudo-inverse of $\mathbf{F}$. It is noted that a set of received sequences $\mathbf{r}_l$ is known from measurements with L observation receivers, while the transmit PA input signals a_{1k} are known by default – however, the sequences a_{2k} are not directly observable. Thus, the PA model coefficients need to be estimated in a recursive manner, due to the recursive definition of the PA model outputs in (1). A least squares-based solution for the estimation is described in Algorithm 1. Here, $\tilde{a}_{2k}$, θ, $\tilde{b}_{2k}$, and $\tilde{r}_l$ are updated (in this order) in each iteration of the algorithm, with tilde referring to local variables, until the error between $\tilde{r}_l$ and the actual measurements r_l is minimized.

Algorithm 1 Proposed iterative least-squares procedure for the identification of dual-input PA model coefficients θ_{kp} from over-the-air measurements with at least two observation receivers. Variables with $\tilde{()}$ are local estimates.

Input: a_{1k}, η_{lk}, λ_{ki}, and $\mathbf{r}_l$
Set initial estimates of PA model output $\tilde{b}_{2k}(0) = 0$
Define desired accuracy $\text{NMSE}_{\text{des}} = 0$
Set initial value $\text{NMSE} = \infty$
while $\text{NMSE} < \text{NMSE}_{\text{des}}$ **do**
    $i = i + 1$
    Use $\tilde{b}_{2k}(i-1)$ in (2) to compute $\tilde{a}_{2k}(i)$
    Use $\tilde{a}_{2k}(i)$ in (12) to compute $\hat{\boldsymbol{\theta}}(i)$
    Use $\tilde{a}_{2k}(i)$ and $\hat{\boldsymbol{\theta}}(i)$ in (9) to compute all $\tilde{b}_{2k}(i)$
    Use $\tilde{b}_{2k}(i)$ in (8) to compute all $\tilde{\mathbf{r}}_l$
    Calculate NMSE = $\max(\text{NMSE}(\mathbf{r}_l, \tilde{\mathbf{r}}_l(i)))$
end while
return PA model coefficients $\hat{\boldsymbol{\theta}} = \hat{\boldsymbol{\theta}}(i)$

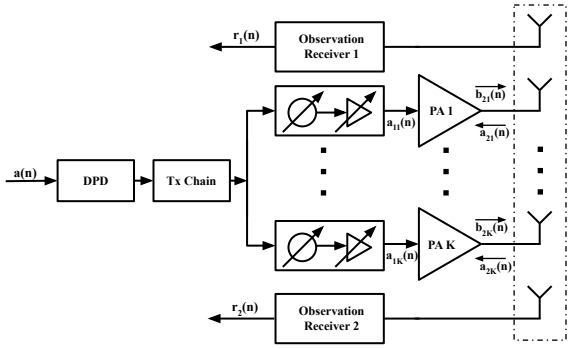

Fig. 2. Illustration of a phased-array transmitter where the first and the last antenna elements of the array are acting as OTA observing antennas for the nonlinear array forward modeling.

Finally, it is noted that with digital MIMO arrays, and thus independent signals in different antenna paths, the estimation system matrix $\mathbf{F}$ is of full rank, with any reasonable modulated sequences, allowing for a unique solution. However, in case of phased-arrays addressed in the forthcoming section, the antenna sequences are highly correlated, and thus additional measures are needed for remedying the involved rank-deficiency.

IV. Application to Phased-Array Linearization

As a concrete example, we next focus on the linearization of millimeter-wave phased-array transmitters, applying the forward model identification solution described in the previous section. Specifically, we assume that a few of the antenna

elements of the transmit array are used for OTA observation purposes, through physical coupling, as illustrated in Fig. 2.

A. Beam-Sweeping Procedure for PA Model Identification

In the phased-array transmitter context with K transmit antennas but only a single input signal $a_{1k} = a \ \forall k$, the regression matrix $\mathbf{F}$ in (11) becomes rank-deficient. To remedy this, we propose a beam-sweeping procedure, where the beam is swept over $M \geq K$ different beamforming angles, using independent input signals, and the measurements and the regressors are simply concatenated to form the new vector $\mathbf{r}$ and matrix $\mathbf{F}$. After doing these steps, PA model identification is performed following the procedure in Algorithm 1. Such beam-formed measurements can in practice be gathered either through a dedicated beam-sweeping period, or alternatively, over time when the base-station is anyway changing the beam from one slot to another for different scheduled users.

B. Per-Beam DPD Learning

We employ an offline direct learning approach to find the optimum DPD coefficients for linearizing the array for a given beamforming direction, or beam index $m \in \{0, 1, ..., M-1\}$. In this approach, the forward path non-linear array model is first identified as described above. Then, the actual DPD system is learned in closed-loop manner as described below.

As for the actual DPD processing model, a simple single-input polynomial model is employed in this work. Denoting the DPD complex baseband input signal by $a(n)$, as illustrated also in Fig. 2, the corresponding DPD output signal $\tilde{a}(n)$ reads

$$\tilde{a}(n) = \sum_{p=0}^{(P_{\text{dpd}}-1)/2} \beta^m_{\text{dpd},p} a^{(p+1)}(n) a^{*p}(n) \qquad (13)$$

The DPD coefficients are denoted by $\beta^m_{\text{dpd},p}$ where p is the nonlinearity order while the superscript m denotes the beam-index within the overall set of available beams.

DPD model parameters are updated by minimizing the error between the input waveform $a(n)$ and the local replica of the intended received signal in beam direction m, which we denote by $\tilde{y}_m(n) = \mathbf{W}^H_m \tilde{\mathbf{b}}_{2,m}(n)$, with $\tilde{\mathbf{b}}_{2,m}(n) = [\tilde{b}_{21,m}(n) \ \tilde{b}_{22,m}(n) ... \tilde{b}_{2K,m}(n)]^T$. The error signal reads

$$e_m(n) = \frac{\tilde{y}_m(n)}{G} - a(n), \qquad (14)$$

where G is the estimated complex linear gain of the forward path, including the array model and the beamforming gain. This error signal contains the information about the residual distortion at the intended receiver, which is then minimized in an iterative fashion, utilizing a gradient-descent type of algorithm. To this end, the self-orthogonalized block-LMS learning rule for the coefficient vector can be formulated as

$$\boldsymbol{\beta}^{m\,*}_{\text{dpd}}(i+1) = \boldsymbol{\beta}^{m\,*}_{\text{dpd}}(i) - \mu \mathbf{R}^{-1} \mathbf{X}^T \mathbf{e}^*_m, \qquad (15)$$

where $\mathbf{X}$ is the regression matrix built from N_{dpd} samples of the input signal $a(n)$, and $\mathbf{R} = E[\mathbf{x}(n)\mathbf{x}^H(n)]$ is the correlation matrix of the DPD input vector $\mathbf{x}(n) = [a(n) \ a^2(n)a^*(n) \ a^3(n)a^{*2}(n)]^T$, shown here for $P_{\text{dpd}} = 5$.

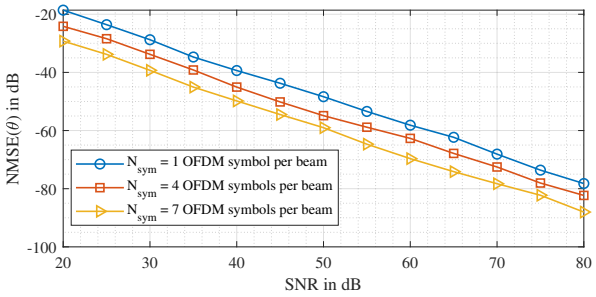

Fig. 3. PA forward model identification performance with $P = 3$ for varying observation SNR and for three different signal lengths per beam.

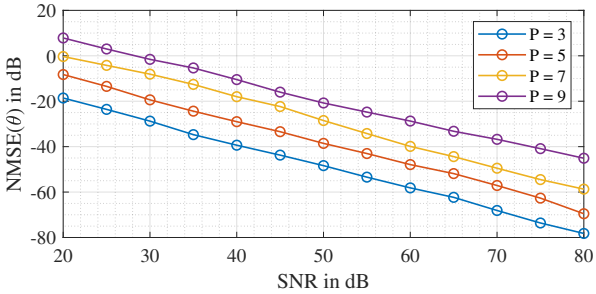

Fig. 4. PA forward model identification performance with $N_{\text{sym}} = 1$ for varying observation SNR and for four different PA model orders P.

V. Numerical Results and Analysis

A. General Evaluation Setup

To assess the performance of the proposed methods, we utilize a set of measured PA coefficients [9] obtained with Anokiwave PAs operating at 28 GHz. These correspond to the α coefficients of the dual-input model in (1). The synthesis of the other dual-input model coefficients β and γ is then done by introducing controlled perturbations to α. To this end, these coefficients are set at 25% strength compared to α, which reflects a realistic load modulation scenario at mmWaves. A 5G NR standard compatible OFDM waveform with 200 MHz bandwidth and 60 kHz sub-carrier spacing is adopted, with an oversampling factor of 4 which allows for both the PA model identification as well as the actual DPD processing and parameter learning. Additional windowing is adopted on top of the baseline OFDM processing to better band-limit the ideal digital waveform. Furthermore, a phased-array transmitter with a total of 16 antennas is considered, of which $K = 14$ are used for transmitting while $L = 2$ antennas are used for observing. In the model identification, the number of considered beams $M = K = 14$ while $N_{\text{sym}} = \{1, 4, 7\}$ OFDM symbols per beam are considered.

B. PA Model Identification Performance

Fig. 3 shows the normalized mean-squared error (NMSE) performance of the proposed PA model identification algorithm for different observation SNR levels, and for fixed PA model order of $P = 3$. The NMSEs are calculated by averaging over 50 Monte Carlo simulations. Further, we study and show the NMSE performance for different polynomial orders of the PA model (P) while keeping the number of OFDM symbols per beam fixed at $N_{sym} = 1$. These results are shown in Fig. 4.

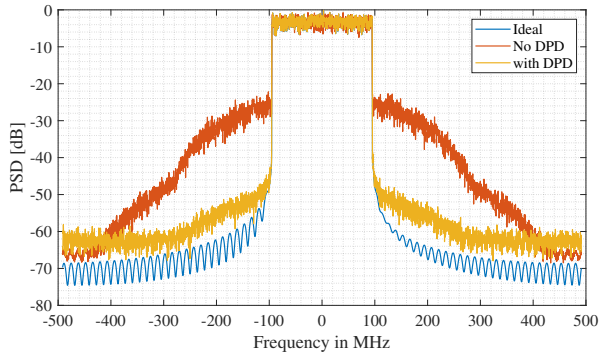

Fig. 5. Linearization example showing the beamformed spectra at far-end user without and with DPD, for PA model estimation NMSE of –30 dB.

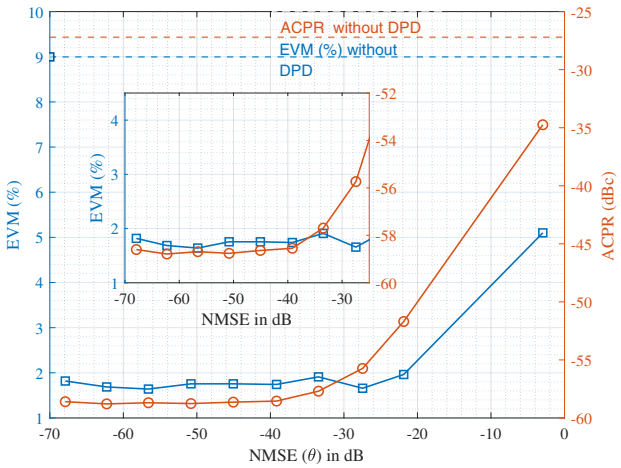

Fig. 6. Linearization performance of the proposed direct-learning DPD system, in terms of EVM (%) and ACPR (in dBc), for different PA forward model estimation NMSEs.

Clearly, larger polynomial order P calls for larger SNR, or alternatively, more OFDM symbols per beam as shown already in Fig. 3. Overall, these results show that acquiring highly accurate forward model estimates is feasible, especially since the observation SNR is typically high [7], [8].

C. DPD Linearization Performance

Next, we assess the actual linearization performance of the proposed DPD approach. We consider an example case with PA model of order $P = 5$ and the DPD model of order $P_{\text{dpd}} = 9$, while otherwise assume the same array transmitter scenario as above. The step-size of the LMS-based learning algorithm in the closed-loop system is set as $\mu = 0.0003$. We first illustrate the linearization performance of the proposed DPD system by plotting the normalized power spectral density (PSD) of the received signal at the far-end user, with and without DPD, for one of the used beams. Such example is shown in Fig. 5, for an identification NMSE of –30 dB, evidencing highly-accurate linearization. Fig. 6 then shows the EVM and the adjacent channel power radio (ACPR) performance of the DPD system for different levels of forward model identification NMSEs, averaged across all the beams. It can be observed that we are able to reach EVM levels in the order of $1.5 - 2.5\,\%$ and ACPR values of around -55 dB to -50 dB under realistic model estimation NMSEs of -30 dB to -20 dB.

VI. Conclusions

In this work, we provided a computationally feasible algorithm and concept to estimate dual-input behavioral models for the individual PA units of an arbitrary active antenna array, under crosstalk, while utilizing only over-the-air observations. Furthermore, a direct-learning mmWave phased-array linearization method was proposed, harnessing the nonlinear array forward modeling stage. Extensive numerical results demonstrated the excellent accuracy of both the forward modeling and the actual linearization methods. Specifically, forward modeling NMSEs in the order of –30 dB and linearization performance reflecting EVMs and ACPRs of around $1.5-2.5\,\%$ and -55 dB to -50 dB, respectively, were shown to be feasible. Our future work will focus on assessing the methods through real-world RF measurements.

References

[1] C. Fager *et al.*, "Linearity and efficiency in 5G transmitters: New techniques for analyzing efficiency, linearity, and linearization in a 5G active antenna transmitter context," *IEEE Microw. Mag.*, vol. 20, no. 5, pp. 35–49, May 2019.

[2] H. Holma, A. Toskala, and T. Nakamura, *5G Technology: 3GPP New Radio*. Wiley, 2019.

[3] D. R. Morgan, Z. Ma, J. Kim, M. G. Zierdt, and J. Pastalan, "A Generalized Memory Polynomial Model for Digital Predistortion of RF Power Amplifiers," *IEEE Trans. Signal Process.*, vol. 54, no. 10, pp. 3852–3860, Oct. 2006.

[4] H. Jiang and P. A. Wilford, "Digital predistortion for power amplifiers using separable functions," *IEEE Trans. Signal Process.*, vol. 58, no. 8, pp. 4121–4130, Aug. 2010.

[5] M. Abdelaziz, L. Anttila, A. Brihuega, F. Tufvesson, and M. Valkama, "Digital predistortion for hybrid MIMO transmitters," *IEEE J. Sel. Topics Signal Process.*, vol. 12, no. 3, pp. 445–454, June 2018.

[6] A. Brihuega *et al.*, "Piecewise digital predistortion for mmwave active antenna arrays: Algorithms and measurements," *IEEE Trans. Microw. Theory Techn.*, vol. 68, no. 9, pp. 4000–4017, Sept. 2020.

[7] X. Wang, Y. Li, C. Yu, W. Hong, and A. Zhu, "Digital predistortion of 5G massive MIMO wireless transmitters based on indirect identification of power amplifier behavior with OTA tests," *IEEE Trans. Microw. Theory Techn.*, vol. 68, no. 1, pp. 316–328, Jan. 2020.

[8] X. Liu, W. Chen, L. Chen, F. M. Ghannouchi, and Z. Feng, "Linearization for hybrid beamforming array utilizing embedded over-the-air diversity feedbacks," *IEEE Trans. Microw. Theory Techn.*, pp. 1–14, 2019.

[9] A. Brihuega *et al.*, "Digital predistortion for multiuser hybrid MIMO at mmwaves," *IEEE Trans. Signal Processing*, vol. 68, pp. 3603–3618, 2020.

[10] N. Tervo *et al.*, "Digital predistortion of phased-array transmitter with shared feedback and far-field calibration," *IEEE Trans. Microw. Theory Techn.*, vol. 69, no. 1, pp. 1000–1015, 2021.

[11] S. Amin, P. N. Landin, P. Händel, and D. Rönnow, "Behavioral Modeling and Linearization of Crosstalk and Memory Effects in RF MIMO Transmitters," *IEEE Trans. Microw. Theory Techn.*, vol. 62, no. 4, pp. 810–823, April 2014.

[12] A. Abdelhafiz *et al.*, "A High-Performance Complexity Reduced Behavioral Model and Digital Predistorter for MIMO Systems With Crosstalk," *IEEE Trans. Commun.*, vol. 64, no. 5, pp. 1996–2004, May 2016.

[13] Z. A. Khan, E. Zenteno, P. Händel, and M. Isaksson, "Digital Predistortion for Joint Mitigation of I/Q Imbalance and MIMO Power Amplifier Distortion," *IEEE Trans. Microw. Theory Techn.*, vol. 65, no. 1, pp. 322–333, Jan. 2017.

[14] K. Hausmair *et al.*, "Digital predistortion for multi-antenna transmitters affected by antenna crosstalk," *IEEE Trans. Microw. Theory Techn.*, vol. 66, no. 3, pp. 1524–1535, March 2018.

[15] C. Fager *et al.*, "Prediction of smart antenna transmitter characteristics using a new behavioral modeling approach," in *2014 IEEE MTT-S International Microwave Symposium (IMS2014)*, 2014, pp. 1–4.

[16] T. Adali, P. J. Schreier, and L. L. Scharf, "Complex-Valued Signal Processing: The Proper Way to Deal With Impropriety," *IEEE Trans. Signal Process.*, vol. 59, no. 11, pp. 5101–5125, 2011.